2013

In Situ Stress Measurement During Aluminum Anodizing Using Phase-Shifting Curvature Interferometry

Ömer Özgür Çapraz
Iowa State University, capraz@iastate.edu

Kurt R. Hebert
Iowa State University, krhebert@iastate.edu

Pranav Shrotriya
Iowa State University, shrotriy@iastate.edu

In Situ Stress Measurement During Aluminum Anodizing Using Phase-Shifting Curvature Interferometry

Abstract
Stress measurements yield insight into technologically relevant deformation and failure mechanisms in electrodeposition, battery reactions, corrosion and anodic oxidation. Aluminum anodizing experiments were performed to demonstrate the effectiveness of phase-shifting curvature interferometry as a new technique for high-resolution in situ stress measurement. This method uses interferometry to monitor surface curvature changes, from which stress evolution is inferred. Phase-shifting of the reflected beams enhanced measurement sensitivity, and the separation of the optical path from the electrochemical cell in the present system provided increased stability. Curvature changes as small as 10−3 km−1 were detected, at least comparable to the resolution of state-of-the-art multiple beam deflectometry. It was demonstrated that small curvature change rates of 10−3 km−1s−1 could be reliably measured, indicating that the technique can be applied to bulk samples. The dependence of the stress change during anodizing on current density (tensile at low current density, but increasingly compressive at higher current densities) was quantitatively consistent with earlier multiple-beam deflectometry measurements. The close similarity between the results of these different high-resolution measurements helps to resolve conflicting reports of anodizing-induced stress changes found in the literature.

Keywords
Mechanical Engineering

Disciplines
Chemical Engineering | Electro-Mechanical Systems

Comments
This article is from *Journal of the Electrochemical Society* 160 (2013): D501–D506, doi:10.1149/2.025311jes. Posted with permission.

Journal of The Electrochemical Society, **160** (11) D501-D506 (2013)
0013-4651/2013/160(11)/D501/6/$31.00 © The Electrochemical Society

In Situ Stress Measurement During Aluminum Anodizing Using Phase-Shifting Curvature Interferometry

Ömer Özgür Çapraz,[a] Kurt R. Hebert,[a,*] and Pranav Shrotriya[b,z]

[a]*Department of Chemical and Biological Engineering, Iowa State University, Ames, Iowa 50011, USA*
[b]*Department of Mechanical Engineering, Iowa State University, Ames, Iowa 50011, USA*

Stress measurements yield insight into technologically relevant deformation and failure mechanisms in electrodeposition, battery reactions, corrosion and anodic oxidation. Aluminum anodizing experiments were performed to demonstrate the effectiveness of phase-shifting curvature interferometry as a new technique for high-resolution in situ stress measurement. This method uses interferometry to monitor surface curvature changes, from which stress evolution is inferred. Phase-shifting of the reflected beams enhanced measurement sensitivity, and the separation of the optical path from the electrochemical cell in the present system provided increased stability. Curvature changes as small as 10^{-3} km^{-1} were detected, at least comparable to the resolution of state-of-the-art multiple beam deflectometry. It was demonstrated that small curvature change rates of 10^{-3} $km^{-1}s^{-1}$ could be reliably measured, indicating that the technique can be applied to bulk samples. The dependence of the stress change during anodizing on current density (tensile at low current density, but increasingly compressive at higher current densities) was quantitatively consistent with earlier multiple-beam deflectometry measurements. The close similarity between the results of these different high-resolution measurements helps to resolve conflicting reports of anodizing-induced stress changes found in the literature.
 [DOI: 10.1149/2.025311jes]

Manuscript submitted July 8, 2013; revised manuscript received September 3, 2013. Published September 16, 2013. This was Paper 966 presented at the Seattle, Washington, Meeting of the Society, May 6–10, 2012.

Measurement of stress evolution has been employed as an integral component in investigations of diverse electrochemical processes such as electrodeposition, anodic oxidation, corrosion, adsorption and lithiation/delithiation in lithium batteries.[1–9] In situ monitoring of the stress state allows direct correlation between stress and the current or potential, thus providing fundamental insight into technologically important deformation and failure mechanisms induced by electrochemical reactions. In the example considered in this work, anodic oxidation of reactive metals such as aluminum and titanium results in buildup of significant levels of stress in the oxide, which may be involved in the development of self-organized arrays of pores.[10–12] In-situ monitoring of stress state can reveal the mechanism by which anodizing produces growth instabilities that initiate development of the porous oxide morphology.

Stress change due to electrochemical reactions is typically inferred from curvature measurements.[13] A reactive sample such as a metal thin film is deposited on one side of a substrate, and stress in the sample leads to substrate bending. Substrate curvature changes can be inferred either using a differential capacitance method or optical deflectometry. In single-beam laser deflectometry, a laser beam is reflected from the substrate and curvature changes are obtained by monitoring the position of the reflected spot.[1–9,14,15] Since stress resolution scales with the square of the substrate thickness, sputtered metallic layers on thin inert wafers are frequently used as samples to maximize resolution.[16,17] Floro and Chason developed an improved version of this technique that relies on monitoring the deflection of an array of equally spaced laser beams reflected from the substrate to measure all components of in-plane substrate curvature with high resolution and robustness.[18] The liquid medium in electrochemical cells imposes restrictions on stress measurements. The integration of the differential capacitance method into electrochemical cells is limited by the electrical conductivity of aqueous media, and hence optical techniques are primarily used for curvature measurement.[19,20] The submerged samples also affect the sensitivity and stability of optical curvature measurement. Optical detectors used to determine beam deflection are usually placed at some distance from the sample, since increasing the sample-detector distance improves curvature resolution.[21] Since the laser beams pass through media of different indexes of refraction, uncertainty in indexes of refraction of liquid can lead to limitation on curvature measurement resolution.[22,23] Also, in cases when optical beams are reflected from the working surface of the sample, reaction-induced hydrodynamic disturbances, such as bubbles and natural convection, may deflect the beams, producing noise and reduced stability of the curvature measurement. Consequently, fully submerged sample configurations that use reactive metal films for beam reflection cannot be used during gas-evolving electrochemical reactions. However, despite these measurement issues, high resolution stress measurements during electrochemical reactions can be achieved by optical deflectometry. Recently, Van Overmere et al. reported a curvature resolution of 0.2 km^{-1} with the multiple beam technique to characterize stress evolution during aluminum anodizing.[22]

In this article we report design and validation of an experimental setup that addresses the limitations of in-situ monitoring of stress evolution in electrochemical cells. For this purpose, we introduce a new high-resolution stress measurement technique for electrochemical systems, phase-shifting curvature interferometry. The experimental design incorporates advantages such that in-situ stress measurement can be performed on both monolithic or layered sample configurations, and curvature measurements are not influenced by hydrodynamic disturbances induced by electrochemical reactions. Aluminum anodizing experiments were used to validate the curvature interferometry method. The literature over the last fifty years contains a number of contradictory observations about stress evolution during Al anodizing, starting with Vermilyea's report that oxidation produced compressive stress.[24] Wüthrich also found that stress change due to barrier oxide formation in neutral solution became increasingly compressive at larger current density.[25,26] However, Nelson and Oriani along with Bradhurst and Leach observed that the stress change during anodizing was compressive at low current density but increasingly tensile at higher current densities.[4,5] Moon and Pyun reported complex trends of stress vs. current density during anodizing in sulfuric acid, but also found tensile stress changes at relatively high current density.[27] Proost and co-workers recently presented the first high-resolution measurements, obtained by multiple beam deflectometry.[6,23,28] They found that the anodizing stress change became more compressive at higher current density, in agreement with the work of Vermilyea and Wüthrich but in contrast with the others. The present work attempts to resolve these contradictory trends by using curvature interferometry to characterize stress evolution during anodizing in phosphoric acid, comparing the results to those of similar experiments by Proost and coworkers. In the rest of the paper, we first provide background on phase-shifting curvature interferometry and describe our experimental design. Then the stability and measurement resolution of the curvature interferometer are demonstrated, and we finally discuss the results of anodizing experiments.

*Electrochemical Society Active Member.
[z]E-mail: shrotriy@iastate.edu

Theory of Phase-Shifting Curvature Interferometry

Phase-shifting curvature interferometry uses an interference measurement to detect changes in the curvature of a sample undergoing treatment. As shown in Fig. 1, the interferometer apparatus consists of a convex lens, a reflecting mirror, and a reflective sample surface arranged such that the sample surface and the mirror are located in the two focal planes of the lens, separated by the focal distance f. The optical system is on the opposite side of the sample from the electrochemical cell. In this arrangement, points D and C on the sample are the images of points A and B, respectively: any beam b_1 incident on point A is also incident on point D, and any beam b_2 incident on point B will also reflect from point C. Thus, both beams are reflected twice from the sample and accumulate a path length difference δ.

The path length difference between the beams is directly related to sample curvature changes. In Fig. 1, reflected beams from points A and B on the sample surface result in a path length difference $2(y_A - y_B)$, and similarly, after reflection from points D and C, beams 1 and 2 develop a path length difference $2(y_D - y_C)$. The total length difference δ between the two beams is

$$\delta = 2(y_A - y_B) + 2(y_D - y_C). \quad [1]$$

The relation of the path length difference to the curvature follows a finite difference approximation,

$$\kappa \approx \frac{d^2y}{dx^2} \approx \frac{1}{d}\left(\frac{y_D - y_C}{c} + \frac{y_A - y_B}{c}\right) = \frac{\delta}{2cd} \quad [2]$$

Here c is the distance between point A and B, the same as the distance between point C and D; d is the distance between the midpoints of the segments $\overline{AB}$ and $\overline{CD}$. Eq. 2 is valid if the sample deflections y_A, y_B, y_D and y_C are small, and the sample is initially flat with negligible slope. The path length difference changes continuously during an experiment in response to stress-dependent curvature changes.

The time-dependent path length difference and hence curvature are measured by interfering the beams. The path length difference $\delta(t)$ introduces a phase shift $\phi(t) = \phi_0 + 2\pi\delta(t)/\lambda$, where λ is the wavelength of the light source and ϕ_0 is the initial phase value of the fringe. The continuously changing phase shift causes the intensity of the interfered beam to oscillate over time according to

$$I(t) = I_m + A\sin\left(\frac{2\pi\delta(t)}{\lambda} + \phi_0\right) \quad [3]$$

where I_m and A are the mean intensity and amplitude of the measured intensity signal. Differentiating this expression produces a relation between changes in path length difference and measured intensity changes,

$$dI = \frac{2\pi A}{\lambda}\cos\left(\frac{2\pi\delta}{\lambda} + \phi_0\right)d\delta \quad [4]$$

However, Eq. 4 cannot be unambiguously inverted to compute the path length change, as the original phase ϕ_0 is not explicitly known. In addition, the sensitivity of the measurement is extremely low when the phase difference between the beams is a multiple of π.

A phase-shifting interferometer provides unambiguous path length measurement and also eliminates phase-dependent sensitivity. In order to implement the phase shift, the beams reflected from the surface are initially split into two components, and a phase shift of 90° is introduced in only one of the components. The interference of the unaltered component produces intensity $I_1(t) = I_{1m} + I_{1\text{var}}(t)$, where $I_{1\text{var}} = A_1\sin[(2\pi\delta/\lambda) + \phi_0]$. Similarly, the interference of the phase-shifting component results in intensity $I_2 = I_{2m} + I_{2\text{var}}(t)$, where $I_{2\text{var}} = A_2\cos[(2\pi\delta/\lambda) + \phi_0]$. Both intensity changes dI_1 and dI_2 are monitored. Combining these measurements leads to an expression for the path length change that does not incorporate the unknown initial phase,

$$d\delta = \frac{\lambda}{2\pi A_1 A_2}(I_{2\text{var}}(t)dI_1 - I_{1\text{var}}(t)dI_2) \quad [5]$$

Changes of path length and curvature are then related by Eq. 2, $d\kappa = d\delta/2cd$.

Stress and curvature changes are related by the Stoney thin film approximation, if the ratio of sample to substrate thickness is small. As discussed below, this restriction was satisfied in our anodizing experiments. According to the Stoney approximation for thin planar specimens with biaxial stress state, the stress change is obtained from

$$dF = \frac{E_s h_s^2}{6(1-\nu_s)}d\kappa \quad [6]$$

where F is the in-plane force per unit width at the Al surface produced by anodizing, h_s is the substrate thickness, and ν_s and E_s are the Poisson's ratio and Young's modulus of the substrate. In terms of the measurement variables, dF is

$$dF = \frac{E_s h_s^2 \lambda}{24\pi(1-\nu_s)cdA_1A_2}(I_{2\text{var}}(t)dI_1 - I_{1\text{var}}(t)dI_2) \quad [7]$$

The force per width is equivalent to the biaxial in-plane stress change σ_{xx} integrated over the thickness dimension,

$$F = \int_0^\infty \sigma_{xx}\,dz \quad [8]$$

where the x-axis lie parallel to the surface, and the z-axis extends toward the bulk metal from its origin on the solution interface. The stress change σ_{xx} may be localized primarily within the sample layer, in which case F can be interpreted as the "stress-thickness product" of the sample, the product of the average in-plane stress in the oxide and its thickness. However, if the substrate is not completely inert, the reaction-induced stress changes may also extend to a thin layer of adjoining substrate material.

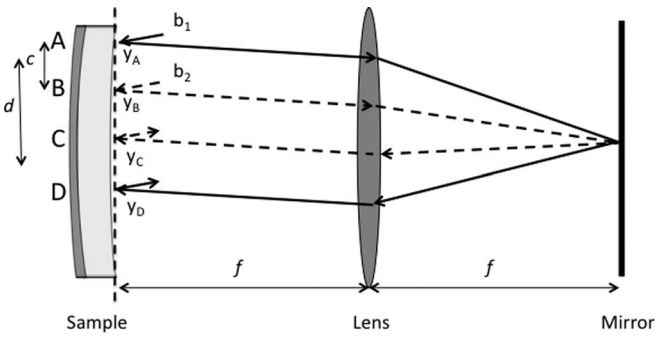

Figure 1. Principle of curvature interferometry. Points A, B, C and D mark the reflections of the two laser beams on the rear surface of the sample; y_A, y_B, y_C and y_D are the horizontal distances at these points between the sample and the reference plane (indicated by the vertical dashed line). c is the spacing between A and B, and d is the distance between the midpoints of $\overline{AB}$ and $\overline{CD}$. f is the focal distance. The reactive surface of the sample in contact with the electrochemical cell is indicated by dark gray shading.

Experimental

Integrated electrochemical cell and interferometry system.— The curvature interferometer was integrated with a specially design electrochemical cell in order to monitor stress development during anodizing. The sample served as one of the walls of the electrochemical cell. Anodizing was confined to the portion of the Al surface in contact with solution, with the optical system on the opposite side of the sample. Since the beam path did not penetrate into solution, bubbles and reaction induced convection flows did not disturb the optical measurements. The Al plate sample was mounted using viscous sealant at its periphery, to allow it to deform while preventing leakage of electrolyte solution. The electrochemical cell and the interferometer were

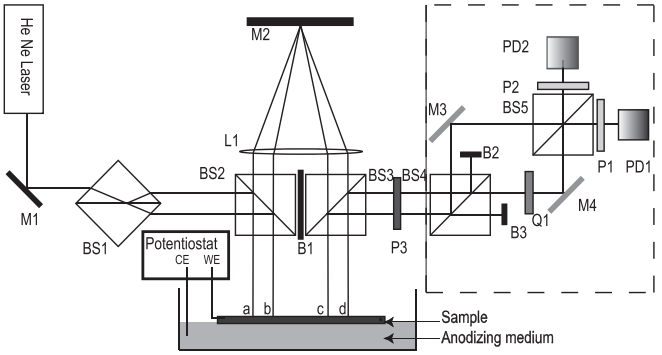

Figure 2. Arrangement of optical components and electrochemical cell. Notation of optical elements is mirror (M), beam splitter (BS), lens (L), beam block (B), quarter wave plate (Q), polarizer (P), and photodetector (PD). The components of the Mach-Zehnder interferometer are enclosed by the dashed line.

enclosed inside an acoustic isolation box and placed on an optical table in order to minimize the influence of acoustic and environmental noise on stress measurements.

The beam paths and components of the optical system are illustrated in Fig. 2. A He-Ne laser ($\lambda = 633$ nm) was used as a light source. A single incident beam from the laser was divided into two parallel beams, using the steering mirror *M1* and the cube beam splitter *BS1*. *BS2* directs both beams to the back surface of the sample, and the reflected beams from points *a* and *b* are then focused onto the mirror *M2* using the convex lens *L1*. After both beams reflect again from points *c* and *d*, *BS3* steers them toward a phase-shifting Mach-Zehnder interferometer in order to determine the path length difference. A suitably oriented quarter-wave plate *Q1* converts the polarization of one of the beams from linear to circular, after which beam splitter *BS5* is used to interfere the two beams. In order to measure the intensity of the interfered beams, linear polarizers *P1* and *P2* are aligned with fast and slow axis of the quarter wave plate respectively, such that output of photodetectors *PD1* and *PD2* are proportional to the sine and cosine of the phase difference. The measured intensities from the two detectors are analyzed using Eq. 5 to monitor path length difference and therefore curvature changes.

Experimental procedures.— Samples were cut into rectangular shape (3.5 × 2.5 cm) from 1 mm thick 99.998% hard aluminum sheet. The Stoney thin-film approximation was satisfied since the anodic oxide thickness of 10–100 nm was much smaller than the Al plate thickness. The cut samples were degreased in acetone and then rinsed in deionized water and dried in an air stream. The surface pretreatment for anodizing involved first etching in 10 wt% NaOH at 60°C for 60 s, followed by immersion in 10-vol% HNO_3 for 30 seconds at room temperature, and rinsing in distilled water.[29] This procedure resulted in linear and reproducible voltage response during anodizing. Reflective mirror-flat gold films were then transferred to the back side of aluminum sample using a template-stripping technique. The positions of the incoming light beams on the sample surface were marked to measure the *c* and *d* values.

At the start of an anodizing experiment, the samples were mounted in the electrochemical cell and the optical system was aligned before introducing solution. In order to determine the stability of the interferometry measurement, in each experiment the curvature of the samples was monitored for three to four hours before introduction of the electrolyte solution. Prior alignment in this manner controlled the exposure time of the Al surface to the phosphoric acid solution. The optical setup was initially perturbed by tapping on the mirror in the Mach-Zehnder interferometer in order to determine the range of intensity changes for the two interfered signals. After perturbation, the samples were left undisturbed for four hours and the curvature changes were monitored to determine the stability and resolution of the curvature measurement.

Anodizing was carried out at ambient temperature in 0.4 M H_3PO_4 solution. Constant current polarization was applied using a two-electrode power supply (Keithley 2400) and platinum wire counter electrode. The current distribution during anodizing is uniform because of the high resistance of the anodic oxide layer relative to the aqueous cell solution. After the anodizing solution was introduced into the electrochemical cell, current was applied and monitoring of voltage and curvature changes initiated. At the conclusion of anodizing, the area of the sample undergoing electrochemical reaction was measured to determine the active area and hence the current density. The current densities in these experiments ranged from 2 to 25 mA/cm^2.

Results and Discussion

Resolution, stability and uncertainty analysis.— The resolution and stability of the interferometry system was demonstrated by measuring its response to a mechanical perturbation. Fig. 3 shows the intensities of the interfered beams measured on a non-reacting sample after the interferometer was initially disturbed by tapping on the steering mirrors. The photodetector outputs are normalized with their amplitudes to facilitate presentation. The effect of the perturbation was seen for the first two hours, as the oscillation due to the tapping disturbances slowly decayed. The plotted outputs clearly demonstrate the phase shift between the two interference signals introduced by the quarter wave plate and polarizers: when one beam was near its peak intensity, the other was between peaks with its intensity changing rapidly. After the influence of the disturbance died out, the interferometer output remained stable for almost six hours of observation. These measurements were performed before each anodizing experiment to verify the stability of the measurement system.

The stable part of the curves in Fig. 3 was analyzed to determine the smallest curvature change that can be reliably measured. Fig. 4 shows the noise level of the curvature measurement, as quantified by the curvature change over each experimental time step determined by Eqs. 2 and 5. Also, Fig. 4 displays the drift of the curvature measurement, indicated by the cumulative curvature change over the stable part of photodetector output in Fig. 3. The curvature changes over individual time steps are all smaller in magnitude than 1×10^{-6} m^{-1}, which may be taken as a noise threshold for the curvature measurement. Over the period of six hours, the drift in the curvature measurement or the cumulative curvature change is less than 1×10^{-4} m^{-1}, indicating that the drift rate of the curvature measurement is approximately 5×10^{-9} m^{-1}s^{-1}.

The stress monitoring setup will primarily be used to determine the change in stress as a function of reaction time, hence uncertainty propagation analysis was also performed to determine the reliability

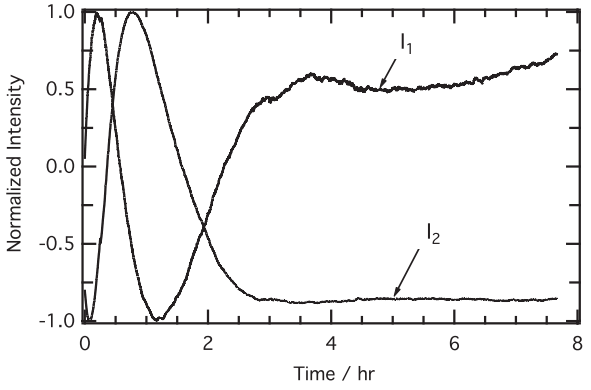

Figure 3. Demonstration of the stability and curvature resolution of the interferometry system. The beam intensities I_1 and I_2 were monitored after mechanical disturbing the system at time zero. Intensities are normalized with the amplitude of the intensity oscillation.

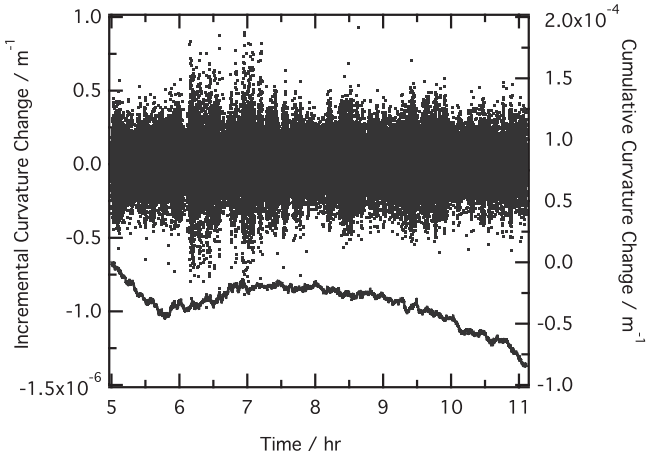

Figure 4. Calculated curvature change at long times during the experiment of Fig. 3. Data points represent incremental curvature change over the interval of 0.4 s between measurements (left axis). The line shows the cumulative curvature change (right axis).

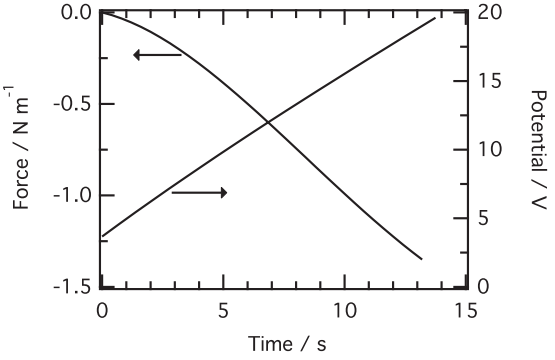

Figure 5. Force change and voltage evolution during Al anodizing at 5 mA cm^2 in 0.4 M H_3PO_4. Negative force change corresponds to compressive stress in the oxide.

of the rate of curvature measurement. From Eq. 2, the rate of curvature change is

$$\frac{d\kappa}{dt} = \frac{1}{2cd}\frac{d\delta}{dt} \qquad [9]$$

Accordingly, the uncertainty in the curvature change rate can be produced by errors in three measurements: the rate of path length change $d\delta/dt$ and c and d, the distances between reflection points (Fig. 1). The uncertainty of $d\kappa/dt$ produced due to each type of error is determined by the partial derivatives of Eq. 9 with respect to these measurements.[30] The overall uncertainty is

$$\Delta\left(\frac{d\kappa}{dt}\right) = \frac{1}{2cd}\left[\left(\Delta\left(\frac{d\delta}{dt}\right)\right)^2 + \left(\frac{d\delta}{dt}\frac{\Delta c}{c}\right)^2 + \left(\frac{d\delta}{dt}\frac{\Delta d}{d}\right)^2\right]^{1/2} \qquad [10]$$

In a similar fashion, the uncertainty of the rate of path length change can be determined as

$$\Delta\left(\frac{d\delta}{dt}\right) = \frac{1}{B}\left[\left(I_{1\mathrm{var}}\Delta\left(\frac{dI_2}{dt}\right)\right)^2 + \left(I_{2\mathrm{var}}\Delta\left(\frac{dI_1}{dt}\right)\right)^2 + \left(\frac{dI_1}{dt}\Delta I_{2\mathrm{var}}\right)^2 + \left(\frac{dI_2}{dt}\Delta I_{1\mathrm{var}}\right)^2\right]^{1/2} \qquad [11]$$

where $B = 2\pi A_1 A_2/\lambda$. The stable parts of the curves in Fig. 3 are used to determine the intensity of the two interfered beams and uncertainty in photodetector output was estimated to be 10 mV. The rates of intensity change were computed using finite difference approximations from the output of the photodetectors, and the uncertainty in the rates of intensity change was estimated from the standard deviation of the computed values. Using these values in Eq. 11, the uncertainty in the rate of path length change was computed to be 0.1 nm/s. The distances c and d were measured using digital calipers, and the uncertainty in the measurement was estimated to be 0.1 mm. From Eq. 10, the uncertainty in the curvature change rate was estimated to be 8×10^{-7} m^{-1}s^{-1}. Thus, in one second a curvature change can be resolved equivalent to a radius change of 1,000 km. In particular, for 1 mm thick aluminum ($\nu_s = 0.33$ and $E_s = 72$ GPa) the stress monitoring system can reliably resolve stress development rates faster than 0.015 Nm^{-1}s^{-1}. Based on previous reports, this resolution of stress development will be adequate to accurately monitor the stress development during aluminum anodizing.

These results indicate that phase-shifting curvature interferometery can determine curvature changes with extremely high resolution and stability. Stability and reliability of the technique are vital for precise in-situ stress measurements. The phase-shifting curvature interferometer enables the unambiguous determination of the path length change between the two beams that are twice reflected from the sample surface and measurement of the time variation of sample surface curvature. The paths of the two beams are arranged to be close to each other in order to minimize the influence of environmental disturbances on the measurement. For the stress-monitoring setup, the use of beams reflected from the back surface of the sample, without passing through the solution, results in extremely stable, reliable and high resolution measurement of curvature changes as seen here.

Stress measurement during anodizing.— Galvanostatic anodizing experiments were carried out to assess the ability of curvature interferometry to measure stress changes during electrochemical reactions. The intensities of the interfered beams were monitored during anodic oxidation, and the integrated stress in the film was determined using Eq. 8. Fig. 5 shows an example of transient potential and stress evolution in these experiments, for the initial 15 s of anodizing at a current density of 5 mA/cm^2. The rate of increase of the integrated stress was 0.1 Nm^{-1}s^{-1}, a factor of ten larger than the minimum measurable rate identified in the previous section. The maximum potential of 20 V reached in this experiment is within the range of stable barrier oxide growth, i. e. below the potential where the pores begins to spontaneously develop.[31] Under such conditions, the electric field in the oxide is approximately constant corresponding to a thickness to voltage ratio $r_A = 1.1$ nm/V.[32] The rate of potential increase dV/dt is

$$\frac{dV}{dt} = \frac{\varepsilon_O i \Omega_{ox}}{6Fr_A} \qquad [12]$$

where ε_O is the anodizing efficiency, i is the applied current density, Ω_{ox} is the molar volume of anodic alumina (33 cm^3/mol) and F is Faraday's constant. The efficiency was calculated to be 0.48 from the approximately linear increase of potential increase of 1.15 V/s in Fig. 4. This value close to the efficiency of 0.47 determined by nuclear reaction analysis of the oxygen content of the film, at the same anodizing conditions.[31] The barrier oxide thickness can then be estimated with reasonable accuracy from the measured potential and the anodizing ratio.

If it is assumed that stress changes due to anodizing are localized entirely in the oxide, the average in-plane stress in the oxide can be calculated from the measured force and the estimated thickness. Van Overmeere et al. used this approach in obtaining the average stress in anodic oxides on Al thin films growth in 0.4 M H_3PO_4.[6,28] and we used the same assumption to directly compare our results with their deflectometry measurements. The apparent average stress during barrier oxide growth was determined by dividing the force per unit width measured at the maximum voltage of 25–30 V by the oxide thickness at this voltage. The oxide thickness calculation accounted for the dependence of the thickness-voltage ratio on current density.[32]

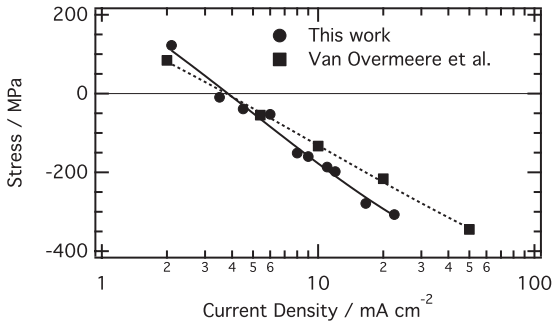

Figure 6. Dependence of the apparent stress in the barrier oxide layer on applied current density. Compressive stress is taken as negative. The average in-plane biaxial stress was computed by dividing the force measurement by the oxide thickness. Results from the present work are compared to those of Van Overmeere et al. obtained with multiple beam deflectometry.[28] Anodizing for all experiments was in 0.4 M H_3PO_4 at ambient temperature.

Fig. 6 shows the resulting average stress values, illustrating a generally high degree of consistency with the deflectometry results of Van Overmeere et al. At the lowest current density of 2 mA/cm^2, both methods found the apparent average stress to be tensile at about 100 MPa. With increasing current density, in both cases the stress increased in the compressive direction, following an approximately logarithmic dependence on current density. Both investigations found a comparable current density of 4 mA/cm^2 at the crossover from tensile to compressive stress. The two sets of results differed mainly in the slope of stress vs. logarithm of current density, −380 and −300 MPa per decade respectively between the present measurements and those of Van Overmeere. The different slopes might be related to the quite different types of metal sample in the two investigations, as Van Overmeere used sputtered Al thin films on silicon, as opposed to hard Al sheets in our work. Thus, possible explanations for the more positive slope in our work might be a tensile stress contribution from the hard Al substrates, or a compressive contribution from the Al thin films. Future work will examine the separate stress changes in the metal and oxide during anodizing.

The high degree of consistency between the deflectometry results of Van Overmeere et al. with the present interferometry measurements, even with different specimen types and configurations, helps to resolve the ambiguous trends reported in the literature on stress changes during anodizing. Earlier stress measurement experiments had required thin metallic foils as substrates (10–100 μm), because the techniques used could not resolve very small curvature changes. These stress measurements may have been influenced by the residual stress and plastic deformation produced during machining of these thin foils, resulting in differing observations. In contrast to the early experiments, both sets of high-resolution measurements agree that anodizing produces compressive stress changes, except at very low current density. Several possible sources of electric field-induced compressive stress are possible during anodizing, including the volume increase due to the anodizing reaction, electrostriction, and field-driven hydration.[10,24,33,34] Effective discrimination between these interpretations requires additional experiments, such as transient interruptions and measurements of stress distributions in the film. Knowledge of stress distributions is also critical to determine the role of stress in transport processes and hence morphological instability.[11]

The results indicate that phase-shifting curvature interferometry can be utilized to measure curvature changes as small as 10^{-3} km^{-1}. In addition, the stability and reliability of the curvature measurement can allow us to resolve curvature change rates as small as 10^{-3} km^{-1}s^{-1}. The optical arrangement of sample and mirror (shown in Fig. 1) ensures that the beams are reflected from the same locations on the sample surface during the curvature measurement. Hence the path length change in the beam is not influenced by surface roughness of the gold film. Phase shifting interferometry allows direct determination of path length change for beam reflected from the gold surface and enables the high-resolution measurement of curvature change. From Eq. 10, the curvature resolution can be improved by increasing the lateral spacing between the beams so the distances c and d in Fig. 1 become larger. Also, since the smallest measurable stress for a given curvature resolution increases with the square of the substrate thickness (Eq. 6), stress resolution can also be improved by decreasing the substrate thickness. It should be pointed out that the substrates used in this work are over four times thicker than those in the high-resolution deflectometry measurements of Van Overmeere et al.[6,23,28] This difference in substrate thickness results in almost an order of magnitude smaller curvature change for thicker substrates, assuming the same stress-thickness product of the barrier oxide film. The stability and high sensitivity of the curvature interferometer allowed accurate resolution of these curvature changes.

Conclusions

Phase-shifting curvature interferometry was integrated in an electrochemical cell to enable high-resolution measurement of stress changes during electrochemical reactions. The results demonstrate the applicability of interferometry approaches in electrochemical systems. The smallest curvature change that could be resolved using the curvature interferometer was 10^{-3} km^{-1}, which is comparable or higher than that obtained by state-of-the-art multiple beam deflectometry techniques. Rates of curvature change as small as 10^{-3} km^{-1}s^{-1} could be reliably measured. This minimum rate is a factor of ten smaller than that needed to resolve stress change rates accompanying anodic oxidation, even with the mm-thick substrates used in this study. The interferometry system should be able to resolve stress changes during extended dissolution processes, where relatively thick samples must be employed. The separation of the optical system and the electrochemical cell ensured that environmental effects on stress measurements were minimized, therefore allowing highly stable measurements. Stress evolution during galvanostatic anodizing of aluminum was performed to demonstrate the effectiveness of the stress monitoring system. The dependence of stress on current density was found to be quantitatively consistent with that observed previously with multiple beam deflectometry.[6,28] Measurements with both methods found that the apparent stress in the barrier oxide was tensile at low current density but became more compressive at higher current density, according to a logarithmic dependence. The close similarity between the results of these two investigations helps to resolve conflicting reports of anodizing-induced stress in the literature.

Acknowledgments

This research was supported financially by the National Science Foundation (CMMI-100748).

References

1. O. E. Kongstein, U. Bertocci, and G. R. Stafford, *J. Electrochem. Soc.*, **152**, C116 (2005).
2. S. J. Hearne and J. A. Floro, *J. Appl. Phys.*, **97**, 014901 (2005).
3. V. Lehmann, *J. Electrochem. Soc.*, **143**, 1313 (1996).
4. D. H. Bradhurst and J. S. L. Leach, *J. Electrochem. Soc.*, **113**, 1245 (1966).
5. J. C. Nelson and R. A. Oriani, *Corros. Sci.*, **34**, 307 (1993).
6. Q. Van Overmeere and J. Proost, *Electrochim. Acta*, **56**, 10507 (2011).
7. K. R. Hebert, J. H. Ai, G. R. Stafford, K. M. Ho, and C. Z. Wang, *Electrochim. Acta*, **56**, 1806 (2011).
8. K. Ueno and M. Seo, *J. Electrochem. Soc.*, **146**, 1496 (1999).
9. V. A. Sethuraman, M. J. Chon, M. Shimshak, V. Srinivasan, and P. R. Guduru, *J. Power Sources*, **195**, 5062 (2010).
10. A. P. Li, F. Müller, A. Birner, K. Nielsch, and U. Gösele, *J. Appl. Phys.*, **84**, 6023 (1998).
11. J. E. Houser and K. R. Hebert, *Nature Mater.*, **8**, 415 (2009).
12. K. R. Hebert, S. P. Albu, I. Paramasivam, and P. Schmuki, *Nat Mater*, **11**, 162 (2012).
13. G. G. Stoney, *P. Roy. Soc. Lond. A. - Conta.*, **82**, 172 (1909).
14. G. S. Sotirovachakarova and S. A. Armyanov, *J. Electrochem. Soc.*, **137**, 3551 (1990).
15. S. N. Sahu, J. Scarminio, and F. Decker, *J. Electrochem. Soc.*, **137**, 1150 (1990).

16. J. Wang, P. Shrotriya, and K. S. Kim, *Experimental Mechanics*, **46**, 39 (2006).
17. P. A. Flinn, D. S. Gardner, and W. D. Nix, *IEEE Trans. Electron Dev.*, **34**, 689 (1987).
18. J. A. Floro and E. Chason, in *In Situ Real-Time Characterization of Thin Films*, O. Auciello and A. R. Krauss Editors, p. 191, Wiley-Interscience, New York (2000).
19. D. Sander and H. Ibach, *Phys Rev B*, **43**, 4263 (1991).
20. T. Heaton and C. Friesen, *Journal of Physical Chemistry C*, **111**, 14433 (2007).
21. G. G. Lang and M. Seo, *J. Electroanal. Chem.*, **490**, 98 (2000).
22. Q. Van Overmeere, J. F. Vanhumbeeck, and J. Proost, *Rev. Sci. Instrum.*, **81** (2010).
23. Q. Van Overmeere, B. Nysten, and J. Proost, *Appl. Phys. Lett.*, **94**, 074103 (2009).
24. D. A. Vermilyea, *J. Electrochem. Soc.*, **110**, 345 (1963).
25. N. Wüthrich, *Electrochim. Acta*, **26**, 1617 (1981).
26. N. Wüthrich, *Electrochim. Acta*, **25**, 819 (1980).
27. S. M. Moon and S. I. Pyun, *Electrochim. Acta*, **43**, 3117 (1998).
28. Q. Van Overmeere, F. Blaffart, and J. Proost, *Electrochem. Commun.*, **12**, 1174 (2010).
29. M. Curioni, P. Skeldon, and G. E. Thompson, *J. Electrochem. Soc.*, **156**, C407 (2009).
30. P. R. Bevington and D. K. Robinson, *Data Reduction and Error Analysis for the Physical Sciences*, McGraw-Hill, Boston (2003).
31. A. Baron-Wiechec, J. J. Ganem, S. J. Garcia-Vergara, P. Skeldon, G. E. Thompson, and I. C. Vickridge, *J. Electrochem. Soc.*, **157**, C399 (2010).
32. Q. Van Overmeere, Ph. D. Thesis, Université Catholique de Louvain, Louvain-la-Neuve, Belgium, p. 153 (2011).
33. N. Sato, *Electrochim. Acta*, **16**, 1683 (1971).
34. R. S. Alwitt, J. Xu, and R. C. McClung, *J. Electrochem. Soc.*, **140**, 1241 (1993).